

Modeling-based Approach Towards Quality by Design for a Telescoped Process

This Zahnd^a, Maja Kandziora^{*b}, Michael K. Levis^b, and Andreas Zogg^{*a}

Abstract: A telescoped, two-step synthesis was investigated by applying Quality by Design principles. A kinetic model consisting of 12 individual reactions was successfully established to describe the synthesis and side reactions. The resulting model predicts the effects of changes in process parameters on total yield and quality. Contour plots were created by varying process parameters and displaying the model predicted process response. The areas in which the process response fulfils predetermined quality requirements are called design spaces. New ranges for process parameters were explored within these design spaces. New conditions were found that increased the robustness of the process and allowed for a considerable reduction of the used amounts of a reagent. Further optimizations, based on the newly generated knowledge, are expected. Improvements can either be direct process improvements or enhancements to control strategies. The developed strategies can also be applied to other processes, enhancing upcoming and preexisting research and development efforts.

Keywords: Continuous process improvement · Kinetic modeling · Quality by design (QbD)



This Zahnd completed his apprenticeship as a chemical laboratory technician in 2014 at Lonza AG. He acquired his BSc in Life Sciences specializing in chemical process technology from the University of Applied Sciences and Arts Northwestern Switzerland (FHNW) in 2022. He is now pursuing an MSc in chemical engineering at FHNW and working in the research group of Dr. Andreas Zogg. Here, his main focus is the

development of a model-based safety concept for continuous ethoxylation.



Dr. rer. nat. Maja Kandziora obtained her PhD in organic chemistry from the Free University of Berlin under the guidance of Prof. Dr. Reissig in 2014. After two post-doctoral stays at University of Basel and Syngenta AG she joined Siegfried AG in 2018 as a Project Manager Process R&D and was responsible for the development of new technologies. In 2023 she became a product chemist at Siegfried AG and is responsible for the scale-up of new processes and the optimization of established ones.



Dr. rer. nat. Michael Karl Levis obtained his PhD in organic chemistry, in 1994, from the Albert Ludwigs University in Freiburg, Germany under the guidance of Prof. Dr. Schmittl and Prof. Dr. Ruchardt. In 1995 he joined Siegfried AG and headed positions in analytical development, chemical development and process optimization including a 3-year internship at the Siegfried site in Pennville, USA. He is the head of

process technologies (R&D) and is principal scientist for particle technologies within the Siegfried group.



Prof. Dr. Andreas Zogg obtained his diploma in technical chemistry (1999) and a PhD in technical science (2003) from the ETH Zurich. After a post-doctoral stay at Ciba SC, he became project leader within the process development department of Ciba SC (2004), polymer additives. In 2009 he joined F. Hoffmann-La Roche AG as a senior scientist in pharma technical development and was responsible for the development

of new technologies as well as technically demanding chemical processes. In 2017 he joined Novartis Pharma AG as safety lab expert in pharma chemical and analytical development. Since 2018 he is a professor for physical chemistry, process modeling and reaction technology at the University of Applied Sciences and Arts (FHNW). His research focuses on the development of new reaction technologies and process modeling approaches for the safe and direct scale-up of chemical processes. Since 2019 he is president and cofounder of the association 'Miniplant 4.0'.

Abbreviations

CQA	Critical quality attributes
NOR	Normal operating range
OFAT	One-Factor-at-a-Time
QbD	Quality by Design
QRPPS	Quality relevant process parameters

1. Introduction

One of the most important focuses in pharmaceutical production is to ensure the safety of the patient. The best way to achieve the required confidence in the production of an API with reproducible quality is extensive and robust process understanding. By developing a mechanistic model for a process, this process understanding can be achieved often with less effort than statistical design of experiment approaches. Additionally, due to the robust

*Correspondence: Dr. M. Kandziora; E-mail maja.kandziora@siegfried.ch

^aInstitute for Chemistry and Bioanalytics, University of Applied Sciences and Arts Northwestern Switzerland, School of Life Sciences (FHNW HLS), Hofackerstrasse 30, CH-4132 Muttenz; ^bSiegfried AG, Untere Brühlstrasse 4, CH-4800 Zofingen

nature of mechanistic models, process optimizations can be made to edge closer to the global optimum.

In this article a two-step telescoped process is investigated and methods to simplify a complex mechanistic model are presented.

1.1 QbD

The ICH guideline Q8 (R2) defines Quality by Design (QbD) as “a systematic approach to pharmaceutical development that begins with predefined objectives and emphasizes product and process understanding and process control, based on sound science and quality risk management”.^[1]

Most important are risks to quality that may directly or indirectly affect the patient. To ensure the quality of drug products these risks must be understood and mitigated. A quality risk assessment is used to evaluate these risks. To achieve this, the significance of quality attributes for a given product needs to be understood. Quality as a combination of attributes that impact the safety and efficacy of the final product. These critical quality attributes (CQAs) need to be identified and their acceptable ranges have to be defined.^[2] Linking the CQAs back to process parameters that can be controlled is achieved by first identifying potential quality relevant process parameters (pQRPPs). These are then investigated to identify the quality relevant process parameters (QRPPs).^[3]

A model is established that describes the effects of the QRPPs on CQAs.^[4,5] This allows the determination of a multidimensional space of QRPP value combinations that are predicted to meet the limits of the CQAs, a so-called design space.

In the traditional approach to process development, one-factor-at-a-time (OFAT), only one process parameter is varied at a time to demonstrate proven acceptable ranges. Normal operating ranges (NORs) are defined within the proven acceptable ranges. The proven acceptable ranges are mostly based on one-factor-at-a-time approach. The robustness of a process investigated by one-factor-at-a-time is only demonstrated for a single parameter varying from the standard process parameters. Fig. 1 illustrates how that creates blind spots for any interacting parameter combinations, even if they are within the investigated ranges.

It follows that applying a QbD approach results in a deeper and more exhaustive understanding of the process. Therefore, wider parameter ranges can be defined, which in turn leads to greater operational flexibility.^[6] Adjustments to reaction conditions, reagents amounts *etc.* within the registered design space can be made without regulatory post-approval.^[1] With additional knowledge and methods becoming available, improvements to the process, the model and control strategies become possible.

1.2 Modeling

An important step in the enhanced QbD approach is the establishment of a model. Its purpose is to link the QRPPs to the CQAs. The model must be able to predict the effects of variations in the process on the product. There are two main concepts to modeling for QbD, mechanistic or empirical. A mechanistic model is derived from known physical and chemical equations. Empirical models on the other hand rely on large amounts of data to find arbitrary equations to describe the investigated process.^[7]

Both concepts have distinct advantages and disadvantages. Mechanistic models tend to be more robust and can be extrapolated to a certain degree as they are based on fundamental equations. However, extensive process knowledge and understanding is required, and the underlying physical and chemical phenomena must be known. This is not the case for empirical models. Therefore, more complex correlations or correlations not yet fundamentally understood can be described. However, this typically requires an extensive experimental design, utilizing statistical methods such as design of experiment.^[8]

1.3 Strategy for Model-based Approach to QbD

The focus of this work is to obtain a better, model-based process understanding, as shown in Fig. 2. Initially the available information and knowledge concerning the investigated process is gathered. Afterwards an initial quality risk assessment is performed. Knowledge gaps that are discovered during this assessment are then used as a basis to define experiments specifically targeted to fill these gaps. Simultaneously, a mechanistic kinetic model is developed. This is based on the available process understanding and represents the working hypothesis. Results from experiments continuously challenge the working hypothesis, and appropriate changes must be made. The model is adjusted and improved accordingly.

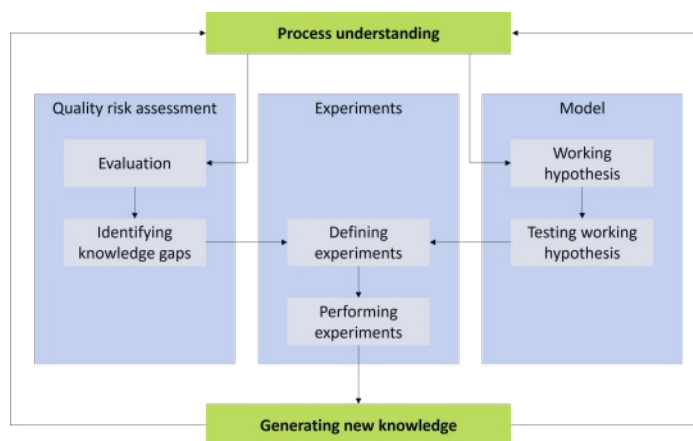


Fig. 2. General strategy for a model-based approach towards QbD.

Reevaluating both the quality risk assessment and the model then restarts this process. This continues until two conditions are met: All potential QRPPs have been investigated and classified as either affecting or not affecting the quality of the product. Additionally, the model must be capable of predicting process responses to a satisfactory degree.

1.4 Investigated Process

The investigated process is a multi-step chemical synthesis of an API. Two telescoped steps of the synthesis are known to be critical for impurity formation. These steps are quite complex and use expensive reagents with an increased chemical hazard potential. As such, these steps are chosen as the subject of this work as

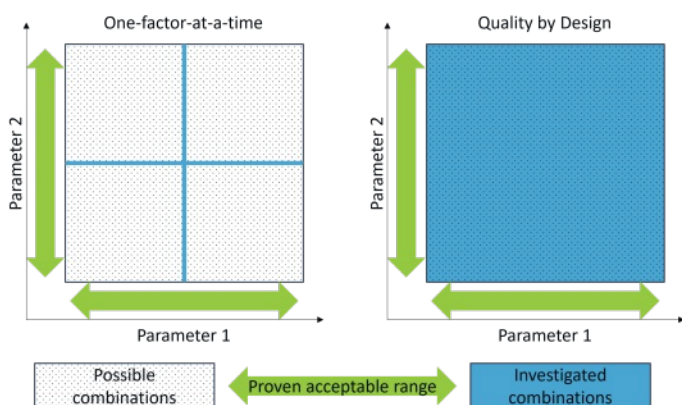
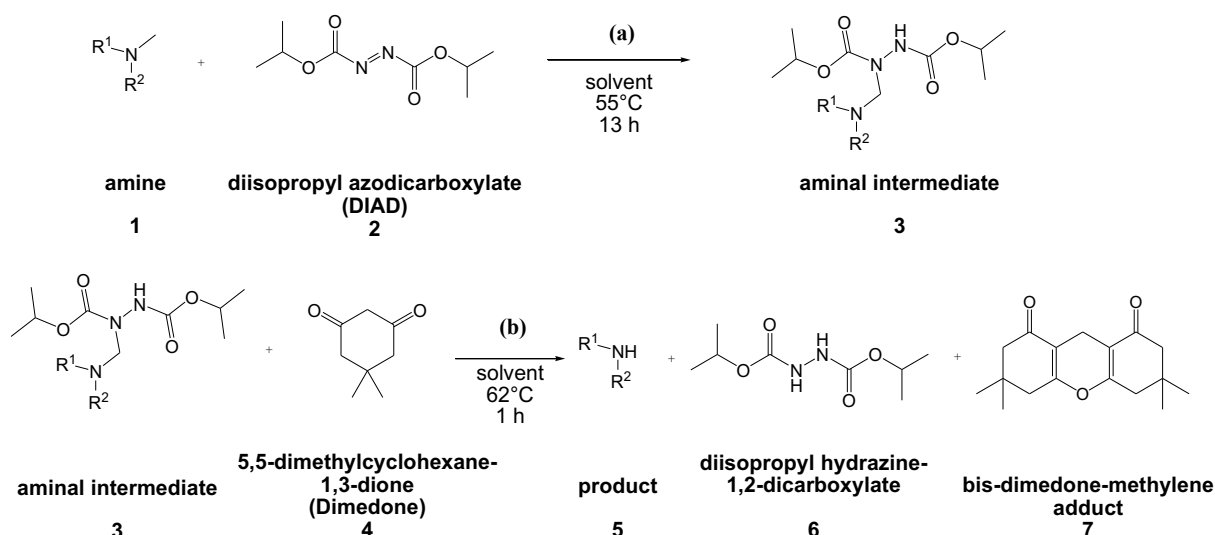


Fig. 1. Comparison of one-factor-at-a-time (left) vs Quality by Design (right) approaches to process development. The blue regions are the investigated/described parameter combinations.

there is potential for optimization of the process and the safety of both the patient and the process.

The two investigated steps are overall an *N*-demethylation in two chemical steps. In the first step a) an amine (**1**) reacts with DIAD (**2**) to form the aminal intermediate (**3**). The second step b) follows without purification. Dimedone (**4**) is used to quench excess DIAD (**2**). Additionally, dimedone (**4**) reacts with the aminal intermediate (**3**) to form the product (**5**) (Scheme 1). The work-up of the resulting suspension is not investigated in this article.



Scheme 1. Overall reaction scheme of the investigated process.

To aid in reproducibility, automation is used whenever possible. The dosing and temperature are controlled using a Mettler Toledo RX-10TM reactor control system. Sampling is performed using a Mettler Toledo EasySampler 1210 system.

2. Results

2.1 Quality Risk Assessment

The first step to assess risks to quality is to define quality in the context of the specific process considered. The process investigated in this article is a telescoped process, where the product is not isolated. Furthermore, only the synthesis and not the purification steps are in the scope of this article. In a telescoped process, a quality risk assessment of the sub-steps can be done to make the assessment more efficient and transparent. The effects of potentially formed impurities on later steps and their purging during purification are not in the scope of this article and therefore, CQAs of the final API like inorganic impurities, polymorphism, residual solvents *etc.* are not described. From prior experience it is however known that impurities formed are purged by a crystallization step.

For these reasons, only yield is defined as an indicator for the CQA 'purity'. Since the starting material (**1**) as well as the product (**6**) is in solution, yield is defined as

$$\text{yield} = \frac{C_{\text{actual}}}{C_{\text{theo,max}}} \cdot 100\% \quad (1)$$

where C_{actual} is the measured concentration of product (**6**) and $C_{\text{theo,max}}$ is the maximum theoretical concentration of product (**6**), based on the concentration of (**1**) in the starting solution.

Yield is not a quality attribute; however, it does serve as a proxy for impurity formation. A higher yield does imply that less side reactions occurred, which may form impurities. With the initial procedure a yield of approximately 80 % is achieved. The design goal is set to 90 % yield for the process optimization. With a traditional approach, the process optimization would have to be performed before validation experiments for the registration of the process. A QbD approach results in a model, which can be used to perform the process optimization *in silico*.

The optimized process then only requires few verification experiments to validate the design spaces and with it the proven acceptable ranges for the registration. This leads to lower experimental effort and therefore saves time and money in research and development.

With the CQA defined, a list of all potential QRPPs is created. To this end the process is divided into subprocesses. These subprocesses are then further divided into individual parameters. This is depicted in an Ishikawa-diagram in Fig. 3.

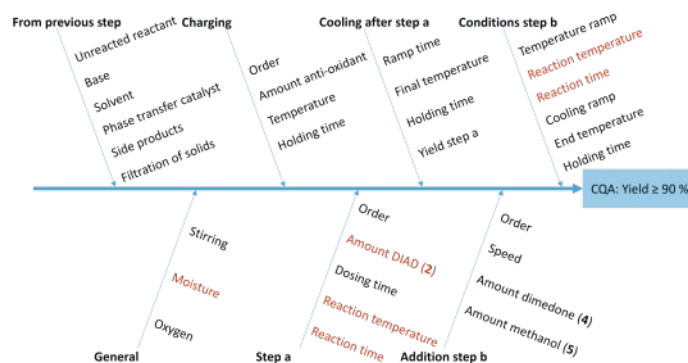


Fig. 3. Ishikawa-Diagram for the quality risk assessment of the investigated process. All potential QRPPs are investigated and if they are found to be quality relevant, they are indicated in red.

The potential QRPPs are then investigated individually to assess if they are relevant QRPPs. For brevity's sake, only a few examples of such investigations are given here.

The starting material is a solution of (1) in solvent from the previous synthesis step (not in the scope of this article). Solids are removed with a filtration, before the solution is used in step a. It is therefore sufficient to demonstrate negligible solubility of side products in the solvent to conclude that they are not quality relevant.

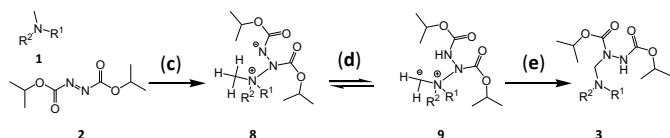
The phase transfer catalyst that is used in the previous step is shown to be readily soluble in the solvent. It is however inert, and the investigated steps a and b are single-phase reactions. Therefore, the phase transfer catalyst is not considered in the model. Similarly, stirring speed is disregarded since the reactions are in a homogeneous phase.

Overall, the 32 potential parameters were reduced to six QRPPs, significantly reducing the model complexity.

2.2 Mechanistic Model

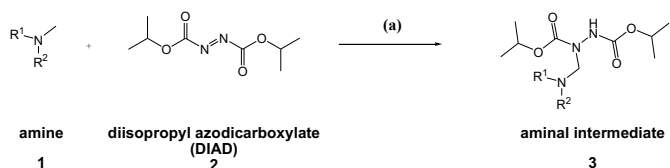
An initial model based on the available knowledge and current hypothesis regarding reaction mechanisms is created, consisting of a total of 36 reactions. Getting all the required kinetic parameters for such an extensive model is time consuming, impractical and in most cases not necessary. In parallel to the quality risk assessment, extensive process understanding was used to simplify the model.

An important method to simplify the model is to consolidate multiple reaction steps into one rate determining step. Scheme 2 shows the proposed reaction mechanism by Huisgen *et al.*^[9] for the aminal (3) formation during step a.



Scheme 2. Proposed reaction mechanism for the aminal formation.^[9]

Three reaction steps for one observable conversion gives the model a lot of degrees of freedom. This leads to issues obtaining a good fit for the kinetic parameters. Instead, the reaction shown in Scheme 3 is used in the model.



Scheme 3. Aminal formation reduced to its rate determining step.

This can be justified as reaction (d) is an intramolecular proton exchange. Reaction (e) is a rearrangement. Both are assumed to be faster than reaction (c) by orders of magnitude, thus making reaction (c) the rate determining step.

For DIAD (2) decomposition is empirically known to occur. However, the decomposition reaction and the resulting compounds are unknown and therefore not described in the initial model. It is however possible to observe the heat of decomposition in DSC measurements. The observed heat flow \dot{Q}_R in W can be described by equation (2):

$$\dot{Q}_R = \Delta H_R \cdot V \cdot v \quad (2)$$

Where ΔH_R is the heat of reaction in J/mole, V is the volume in m³ of the sample, and v is the reaction rate in mole/s/m³ according to equation (3).^[10]

$$v = [\text{DIAD}] \cdot A \cdot e^{-\frac{E_a}{R \cdot T}} \quad (3)$$

Where [DIAD] is the concentration of DIAD (2) in mole/m³, A is the frequency factor in s⁻¹, E_a is the activation energy in J/mole, R is the gas constant in J/K/mole, and T is the temperature in K.

Since the measurement is performed non-isothermally, both kinetic parameters A and E_a can be fitted to one experiment. This is achieved by imposing the experimental temperature-time curve and defining the initial sample. Then the kinetic parameters are adjusted until the simulated heat flow matches the measurement. An overlay of the resulting heat flow-time curves is shown in Fig. 4. To satisfy the mass balance in the model, a decomposition product with molecular weight equal to the product (5) is introduced.

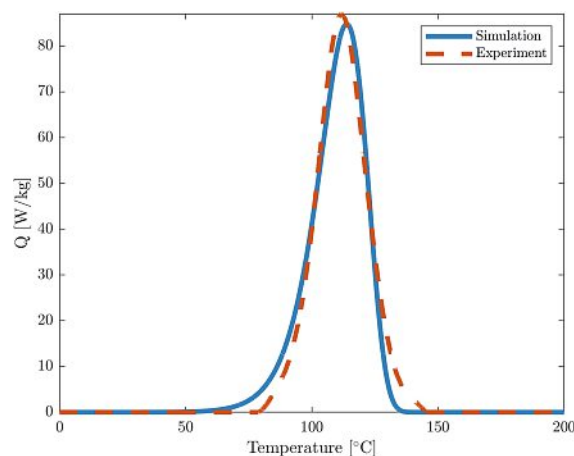


Fig. 4. Experimental DSC data for the DIAD (2) decomposition in orange dashed line and a comparison to the simulated curve using the fitted kinetic parameters in blue.

Besides other specific experiments, where only parts of the process are investigated, experiments with all reaction components are also performed. To gain as much knowledge as possible, experiments are performed far away from the initial setpoints. For example, halving the amount of a reactant used will have a significant effect on the process and help to determine the order of component of the reaction.^[11] A model that can predict even such drastic changes is in turn very robust.

Finally, a model consisting of 12 reactions is established. In Fig. 5 a comparison between model predictions and experimental data is shown. With the available analytical methods, only the starting material (1) concentration can be measured during step a. Similarly, only product (5) concentration can be measured during step b. Additionally, the water (12) content is measured at the start, before the dimeredone (4) addition and after the completed reaction using Karl-Fischer titration. The model can predict the starting material (1) and the product (5) concentration well. The prediction for water (11) content is less reliable, especially for step b. The water (11) concentration is important for step a because it can react with starting material (1) and to the product (5) according to Scheme 4. The following dimerization and condensation reactions are shown in Scheme 5.^[12]

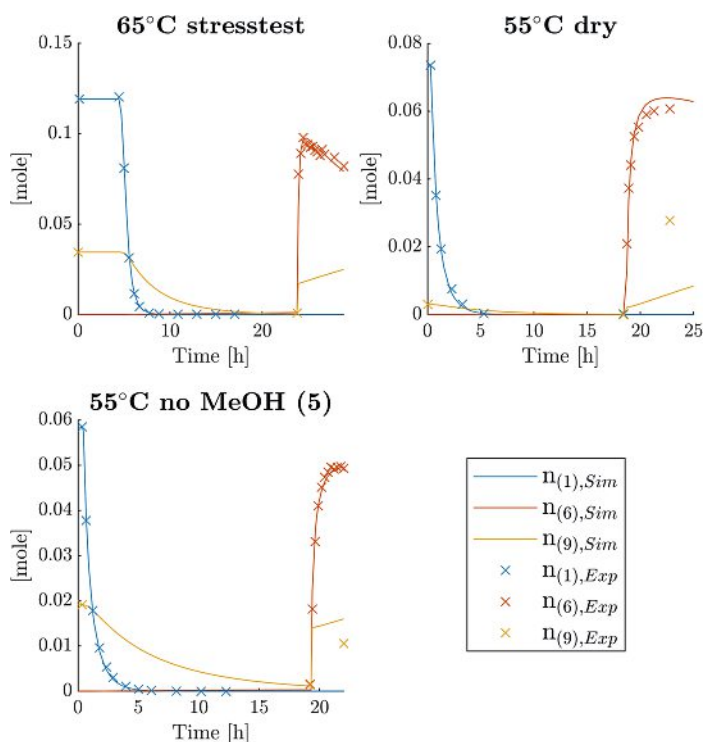
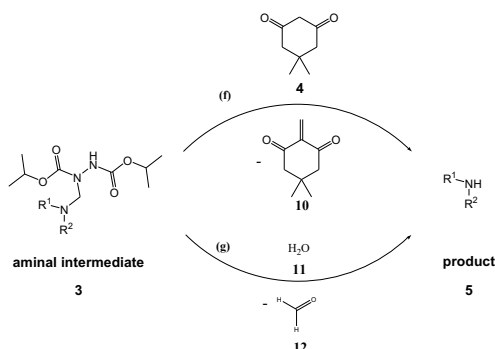
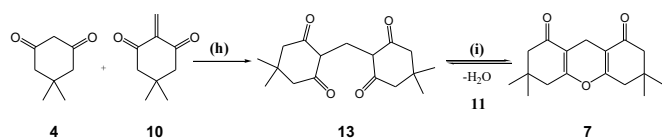


Fig. 5. Comparison of simulated concentration time curves and experimental data for starting material (1), product (6) and water (11) of some selected experiments.



Scheme 4. Reaction (f): formation of product (5) and dimedone-derivative (10) with dimedone (4). Reaction (g): Hydrolyzation of aminal intermediate (3) to product (5) and formaldehyde (12)



Scheme 5. Reaction (h): Dimerization of the dimedone-derivative (10) and dimedone (4). Reaction (i): Condensation of the dimer (10) to (7) and water (11)

This is however deemed acceptable, as the main effects of water (11) in the process are during step a, where water (11) content is well predicted.

2.3 Design Spaces

At this point, the CQAs and the QRPPs are defined, and a model of the process is also established. Critical process parameters were identified. With the model, combinations of variable QRPPs can be found that fulfil the predefined CQA limits. The

space of such parameter combinations is called design space. A design space describes how process parameters or material attributes affect a critical quality attribute.^[1] For the investigated process that means visualizing the effects of the six identified QRPPs on the proxy quality attribute yield. The visualization is done by simulating the process with varying parameter combinations and plotting the process responses in contour plots. The design space is then readily found in the contour plots in the areas that fulfil our design goal of a minimum of 90 % yield. Then an optimum is searched within the design space and the normal operating ranges set.

N-dimensional investigations are difficult to visualize and interpret. Reasonably, only two process parameters and one process response can be investigated per contour plot. It can be a challenge to choose appropriate parameters and responses.

2.3.1 Reaction Temperature

Increasing the reaction temperature not only speeds up the desired reactions, but also side reactions and decompositions. It can be seen in Fig. 6 that an increase in reaction temperature from 55 °C to 65 °C results in a smaller high yield area. Decreasing the reaction temperature to 45 °C instead leads to longer reaction times. The reaction temperature is fixed to 55 °C as a compromise between reaction speed and process robustness.

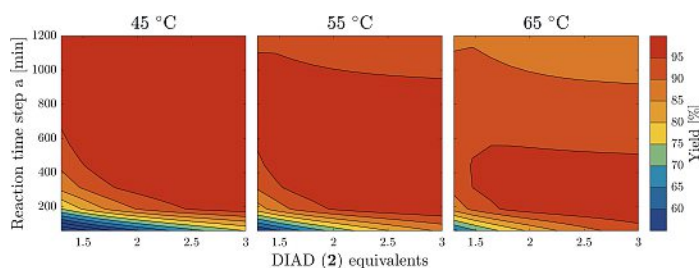
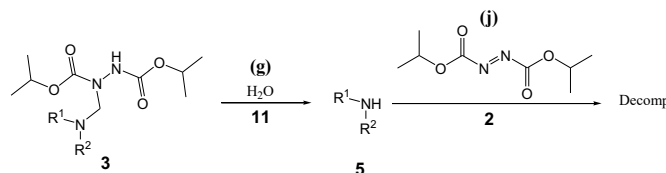


Fig. 6. Contour plots illustrating the effects of reaction time in step a, and DIAD (2) equivalents on yield. At a reaction temperature of 45 °C (left), 55 °C (middle) and 65 °C (right) respectively.

2.3.2 Water Content

During this work, it became clear that water (11) has a significant impact on step a. It reacts with the aminal-intermediate (3) to form the product (5) which is not stable under these conditions according to Scheme 6.



Scheme 6. Reaction (g): Formation of product (5) with water (11) during step a. Reaction (j): Decomposition reaction of product (5) with DIAD (2).

The product (5) loss due to water (11) is illustrated in Fig. 7.

The starting solution produced in a previous chemical step had a water (11) content of up to 0.25 %. The raw material specifications are therefore defined to rule out higher water (11) contents. As such, water (11) content is fixed at 0.25 % as a worst-case scenario for all following contour plots.

2.3.3 DIAD and Reaction Time

The only remaining QRPPs left for step a are the reaction time and the DIAD (2) equivalents. The yield of aminal-intermediate (3) is chosen as the process response. The resulting contour-plot

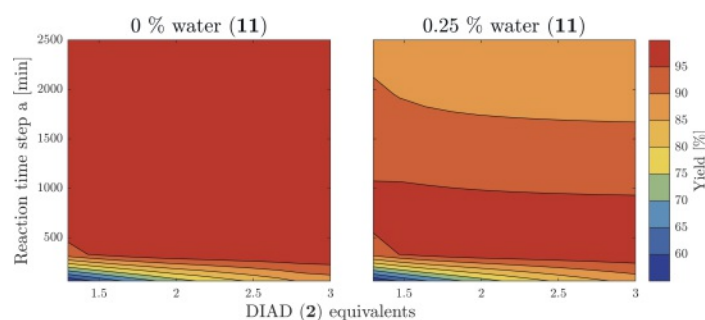


Fig. 7. Contour plots illustrating the effects of reaction time and DIAD (2) equivalents on the yield of water (11) with a content of 0 % (left) and 0.25 % (right). Simulations are performed with a reaction temperature of 55 °C.

is shown in Fig. 8. No data is available for DIAD (2) equivalents lower than 1.5. To avoid incorrect extrapolation as an error source, lower DIAD (2) equivalents were not considered in the design space. The design space is further limited by the design goal of 90% yield.

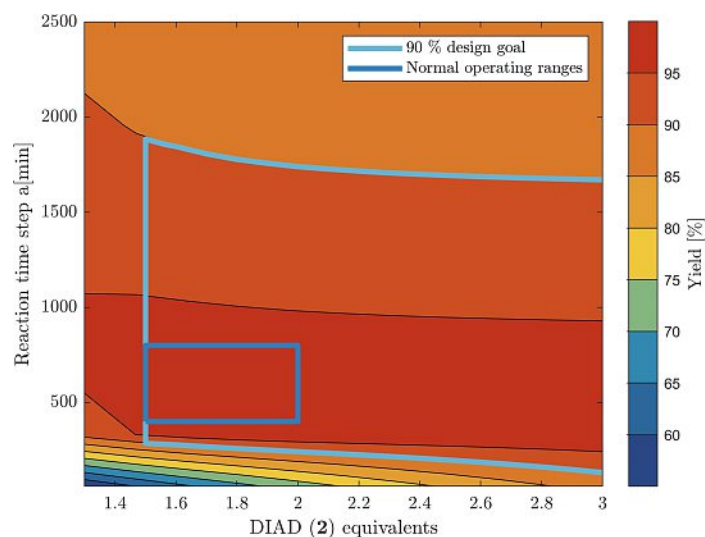


Fig. 8. Contour plot illustrating the effects of reaction time during step a, and DIAD (2) equivalents on the yield. Simulations are performed with a reaction temperature of 55 °C and a water (11) content of 0.25 %.

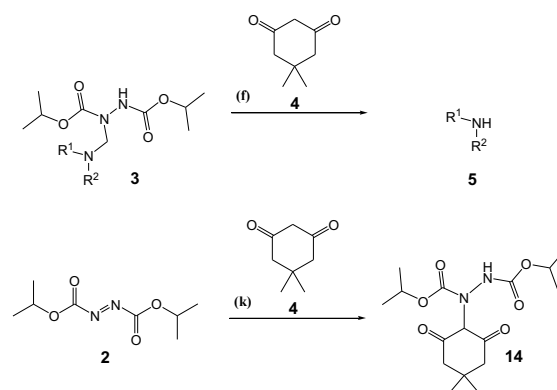
Additional considerations are then made to establish normal operating ranges. With the safety of the product ensured, economic factors can be considered. As such, normal operating ranges are chosen towards lower DIAD (2) equivalents and shorter reaction times.

2.3.4 Dimedone

Dimedone (4) has two functions in the reaction as shown in Scheme 7. It quenches the excess DIAD (2) in reaction (k), while also reacting with the aminal-intermediate (3) to form product (5) in reaction (f). It was found that DIAD (2) decomposes the product (5). However, reaction (k) is orders of magnitude faster than reaction (f). Therefore, not a lot of product (5) decomposition, according to reaction (k), is expected if high enough dimedone (4) equivalents are used.

It can be summarized, that the dimedone (4) amount used has a significant impact on the process and is dependent on the DIAD (2) excess.

To isolate this important interaction, 'max yield' is selected as an alternative process response. This is the highest yield predicted at any timepoint in the model, effectively eliminating the reaction



Scheme 7. Reaction (f): Product (5) formation from aminal intermediate (3) with dimedone (4). Reaction (k): Quench of excess DIAD (2) with dimedone (4).

time as a factor. The resulting contour plot is shown in Fig. 9. The design space is again limited by the design goal of 90% yield and the normal operating ranges are chosen towards lower dimedone equivalents.

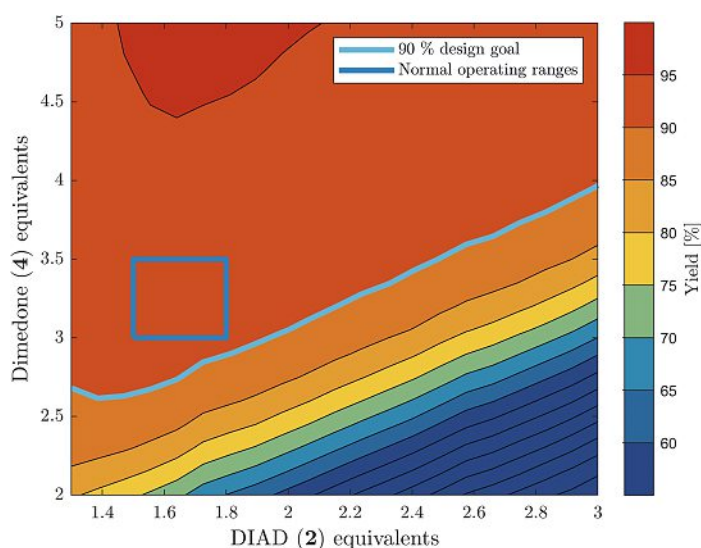


Fig. 9. Contour plot illustrating the effects of DIAD (2) and dimedone (4) eq. with max yield as the process response. Simulations are performed with a reaction temperature of 55 °C, a water (11) content of 0.25 % and a reaction time in step a of 10 h.

2.3.5 Reaction Time Step b

To investigate the reaction time, either the dimedone (4) or the DIAD (2) equivalents must be fixed for each design space. As previously stated, these interacting factors are highly dependent on each other and have drastic effects in step b. Fig. 10 shows contour plots of dimedone (4) equivalents against reaction time at 3 different levels of DIAD (2) equivalents. Higher DIAD (2) equivalents lead to a smaller high-yield window. As such, the design space is established with 1.8 equivalents of DIAD (2), as this is the upper limit of the previously established normal operating range.

2.3.6 Verification

The established design spaces and NORs must be verified, as they are based on model predictions. The number of verification experiments can be limited by forcing unfavorable interactions of the QRPPs. For example, the combination of short reaction times and low DIAD (2) equivalents leads to an incomplete reaction.

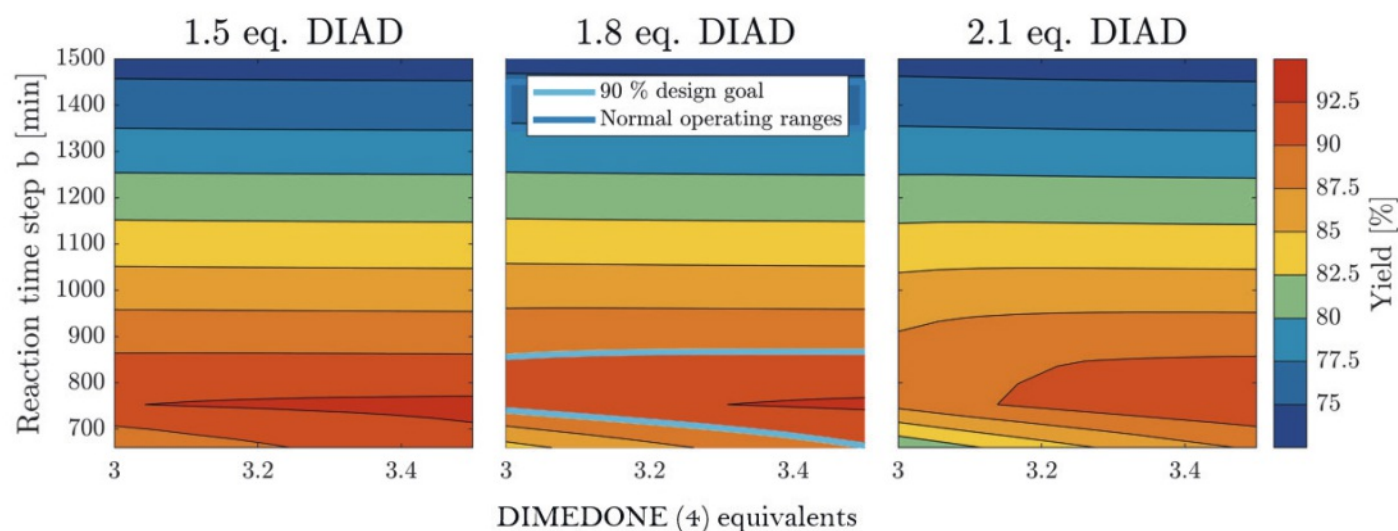


Fig. 10. Contour plots of total reaction time and dimedone equivalents with yield as the process response with 1.5, 1.8 and 2.1 equivalents of DIAD, (2), respectively.

The opposite, long reaction times and high DIAD (2) equivalents, leads to increased decomposition reactions. Now, if the CQA limits are fulfilled in both these extreme cases, then less extreme cases would not need to be verified.

Over the course of an QbD approach, a sufficient process understanding is to be expected. A quite generic example for such a correlation is reaction time and temperature. A long reaction time and a high temperature ensures a completed reaction, but in turn results in increased thermal stress for the product. The inverse, *i.e.* short reaction time and low temperature, would reduce thermal stress but risk incomplete reaction.

3. Conclusion

A mechanistic model for the investigated process is successfully developed. The QbD approach forces an in-depth investigation of the process, which leads to significantly increased process understanding. Thanks to the systematic approach of a quality risk assessment previously unknown effects are investigated. It is discovered that moisture is critical and leads to increased decomposition reactions. These effects are described in a model, which allows for new control strategies. The very complex interactions and relationships between the many critical process parameters would not have been discovered by applying the traditional OFAT approach.

Furthermore, improvements to the process are enabled. A significant reduction in DIAD (2) equivalents was made and is already implemented at the commercial stage. Not only is this an economic improvement, but also improves process safety, as DIAD (2) has an increased chemical hazard potential.

With more data collected from the production scale, further improvements will be possible in the future. The additional regulatory freedom granted would enable easier implementation of these improvements.

Overall, applying mechanistic modeling to QbD results in robust process understanding, while not requiring extensive experimental designs. This means fast process optimization and an enhanced control over quality.

Acknowledgements

The author would like to thank Siegfried AG for hosting the thesis on which this article is based on. To all the Siegfried lab technicians that contributed to this work, and especially Ines Oberhuber for her practical support.

- [1] 'ICH guideline Q8 (R2) on pharmaceutical development', EMA, 2017.
- [2] 'ICH guideline Q9 on quality risk management', EMA, 2015.
- [3] Y. Abe, K. Emori, *Org. Process Res. Dev.* **2022**, *26*, 43, <https://doi.org/10.1021/acs.oprd.1c00145>.
- [4] 'ICH-Endorsed Guide for ICH Q8/Q9/Q10 Implementation', ICH, 2010.
- [5] Y. Abe, K. Emori, *Org. Process Res. Dev.* **2022**, *26*, 56, <https://doi.org/10.1021/acs.oprd.1c00146>.
- [6] A. G. Lolas, A. S. Rathore, *BioPharm Int.* **2012**, *25*, <https://doi.org/10.1002/9780470466315>.
- [7] J. Djuris, Z. Djuric, *Int. J.Pharm.* **2017**, *533*, 346, <https://doi.org/10.1016/j.ijpharm.2017.05.070>.
- [8] S. N. Politis, P. Colombo, G. Colombo, D. M. Rekkas, *Drug Dev. Ind. Pharm.* **2017**, *43*, 889, <https://doi.org/10.1080/03639045.2017.1291672>.
- [9] R. Huisgen, F. Jakob, *Justus Liebigs Ann. Chem.* **1954**, *590*, 37, <https://doi.org/10.1002/jlac.19545900103>.
- [10] M. Elrod, *J. Chem. Educ.* **2005**, *82*, 40, <https://doi.org/10.1021/ed082p40>.
- [11] J. Burés, *Angew. Chem. Int. Ed.* **2016**, *55*, 16084, <https://doi.org/10.1002/anie.201609757>.
- [12] H. Naeimi, Z. S. Nazifi, *J. Ind. Eng. Chem.* **2014**, *20*, 1043, <https://doi.org/10.1016/j.jiec.2013.06.041>.

License and Terms



This is an Open Access article under the terms of the Creative Commons Attribution License CC BY 4.0. The material may not be used for commercial purposes.

The license is subject to the CHIMIA terms and conditions: (<https://chimia.ch/chimia/about>).

The definitive version of this article is the electronic one that can be found at <https://doi.org/10.2533/chimia.2024.135>